Paper-based capacitive sensors for identification and quantification of chemicals at the point of care

Jie Hu[a,b,1], Chee-Hong Takahiro Yew[b,c,1], Xiaoshuang Chen[b,1,2], Shangsheng Feng[b,d,e], Qu Yang[b], Shuqi Wang[f,g,h], Wei-Hong Wee[b,c], Belinda Pingguan-Murphy[c], Tian Jian Lu[b,*], Feng Xu[a,b,**]

[a] MOE Key Laboratory of Biomedical Information Engineering, School of Life Science and Technology, Xi'an Jiaotong University, Xi'an 710049, China
[b] Bioinspired Engineering and Biomechanics Center (BEBC), Xi'an Jiaotong University, Xi'an 710049, China
[c] Department of Biomedical Engineering, Faculty of Engineering, University of Malaya, Kuala Lumpur 50603, Malaysia
[d] MOE Key Laboratory for Multifunctional Materials and Structures (LMMS), School of Aerospace, Xi'an Jiaotong University, Xi'an 710049, China
[e] State Key Laboratory of Mechanical Structure Strength and Vibration, School of Aerospace, Xi'an Jiaotong University, Xi'an 710049, China
[f] State Key Laboratory for Diagnosis and Treatment of Infectious Diseases, First Affiliated Hospital, College of Medicine, Zhejiang University, Hangzhou 310003, China
[g] Collaborative Innovation Center for Diagnosis and Treatment of Infectious Diseases, Hangzhou 310058, China
[h] Institute for Translational Medicine, Zhejiang University, Hangzhou 310029, China

ARTICLE INFO

ABSTRACT

The identification and quantification of chemicals play a vital role in evaluation and surveillance of environmental health and safety. However, current techniques usually depend on costly equipment, professional staff, and/or essential infrastructure, limiting their accessibility. In this work, we develop paper-based capacitive sensors (PCSs) that allow simple, rapid identification and quantification of various chemicals from microliter size samples with the aid of a handheld multimeter. PCSs are low-cost parallel-plate capacitors (~ $0.01 per sensor) assembled from layers of aluminum foil and filter paper via double-sided tape. The developed PCSs can identify different kinds of fluids (*e.g.*, organic chemicals) and quantify diverse concentrations of substances (*e.g.*, heavy metal ions) based on differences in dielectric properties, including capacitance, frequency spectrum, and dielectric loss tangent. The PCS-based method enables chemical identification and quantification to take place much cheaply, simply, and quickly at the point-of-care (POC), holding great promise for environmental monitoring in resource-limited settings.

1. Introduction

The identification and quantification of chemical substances (*e.g.*, heavy metal ions and organic chemicals) are not only of significant importance in scientific communities, but also draw extensive interest from the general population in terms of social activities and environmental surveillance [1–4]. For example, water contaminated with heavy metal ions or organic chemical compounds may not only be directly harmful to human beings, but can also cause severe illnesses through bioaccumulation [4,5]. Current standard laboratory methods for the identification and quantification of these contaminants require large and expensive equipment, such as atomic absorption spectrometry and inductively-coupled plasma mass spectrometry for the analysis of heavy metal ions [4], or liquid chromatography coupled

with mass spectrometry for the measurement of organic chemical compounds [5]. Although these methods offer high specificity and sensitivity, they require bulky equipment and professional staff, which is labour-intensive, time-consuming, high-cost as well as hard to transport, thus hindering their in-field and on-site applications, especially in resource-limited settings (where there nevertheless exists a great demand). Currently, 42% of the global population still has no access to piped drinking water on premises, and 9% (*i.e.*, 663 million people) lack access to an improved water source and have to use water from rivers, springs, lakes, or wells directly [6,7]. These unimproved surface water sources are susceptible to pollution from factory farms, industrial plants and human activities, which makes dirty water the top health risk in developing countries, and also a threat to both quality of life and public health in developed countries (*e.g.*, USA, see http://

---

www.nrdc.org/water/). Therefore, there is an increasing need to develop low-cost and simple methods for chemical detection (identification and quantification) to monitor water contamination for human health and safety at the point of care (POC).

The strategy to identify and quantify chemical substances is generally by transducing the target to a readable or measurable mechanical, thermal, sonic, optical, electronic or magnetic signal and further to employ a readout system to interface with the signal [8]. Thanks to the rapid advances in microfluidics and nanotechnology, the signal transformation now can be realized in integrated and miniaturized devices, such as plasmonic technology [8,9], gold nanoparticle-implemented microfluidics [10], and fluorescent nanomaterial and related systems [11]. Although these methods can provide sensitivity and specificity comparable to bulky equipment, they are not convenient to operate by end-users since they still depend on laboratory-based instruments for result analysis, such as a Raman spectrometer or a fluorescent microscope. Recently, Lu and co-authors have reported that using a commercially-available personal glucose meter detects many non-glucose targets in a single step, which is a good example in development of point-of-care testing (POCT) [12,13]. Meanwhile, nanotechnology- and/or microfluidics-based diagnostic paper tests are simple to design, easy to prepare and robust to utilize, and thus have attracted increasing interest for POCT [14,15]. Paper-based diagnostic devices have so far achieved success in several applications, including home pregnancy tests, blood glucose metering, and so on [16]. Therefore, there is increasing interest in developing paper-based sensors for applications related to human healthcare and environmental monitoring.

Currently, paper-based diagnostic devices have been developed to detect heavy metal ions based on electrochemical [17], fluorescent [18], and colorimetric strategies [19–21]. Most of these strategies are designed to analyse a specific heavy metal ion. One of these strategies, using DNA-based fluorescent chemosensors on microbeads, is able to discriminate eight heavy metal ions with high selectivity and sensitivity [4]. However, it takes a long incubation time (2 h, or even 24 h) and requires statistical analysis for pattern-based responses, which may limit its applications at the POC. Identification of organic chemical compounds using paper-based devices has not yet been explored. However, electrical signals, especially dielectric performances, have been explored to identify and quantify substances for chemical and biological sensing, including water [22,23], volatile organic compounds [3,24,25], protein biomarkers [26–31], nucleic acids [32–34], microorganisms [35,36], and even biotin-streptavidin binding [37]. This has demonstrated that dielectric performance can be used as a versatile marker for chemical detection. However, these existing methods require complicated design and fabrication procedures [3,23–25,37] and refined chemical modification and preparation [26–36], or show very limited potential application (i.e., relative humidity sensing) [22]. Therefore, there is still an unmet need for a low-cost, convenient, disposable and general way to identify and quantify solutions, whether they are homogenous (e.g., pure organic chemical liquids) or heterogeneous (e.g., heavy metal salt solutions).

In this study, we developed low-cost paper-based capacitive sensors (PCSs) for identification and quantification of chemicals based on their dielectric properties at the POC. Different chemicals have different structures and thus provide characteristic dielectric properties, including capacitance, frequency spectrum, and dielectric loss tangent (tanδ), which may be used for chemical identification and concentration quantification. On the other hand, many instruments exist for analysis of the above dielectric properties, including multimeters, impedance analyzers, network analyzers, and dielectric spectrometers, making various levels of measurement possible. In the present study, we first investigated the effects of various factors on the performance of PCSs, including geometric structures of PCSs, sample loading volume, measuring instruments, measurement positions, status of samples (wet or dry) on PCSs, and environmental conditions (temperature

and relative humidity). Subsequently, we proved the concept that the PCSs had the capability for identification (mainly for organic chemical compounds) and quantification (organic and salt solutions) of chemicals at the POC. The developed PCSs are easy to prepare and simple to use, thus holding great promise for environmental monitoring.

2. Materials and methods

2.1. Chemicals & Reagents

Filter paper (No. 201, Φ18 cm) was obtained from Hangzhou Whatman-Xinhua Filter Paper Co., LTD. (Hangzhou, China). Aluminum foil was obtained from Beijing Mengyimei Trade Center (Beijing, China). Double-sided tape (Scotch® Core Series XQ) was obtained from 3 M (Minnesota, USA). $NaNO_3$, KNO_3, $Fe(NO_3)_3$, $Na_2B_4O_7$, hydrogen peroxide (30% v/v), methanol (MeOH), ethanol (EtOH), isopropyl alcohol (iPrOH), glycerol, ethyl acetate (EA), dimethyl sulfoxide (DMSO) and tetrahydrofuran (THF) were obtained from Tianjin Zhiyuan Chemical Reagent Co., LTD. (Tianjin, China). NaCl, Na_2SO_4, $NaHCO_3$, NaH_2PO_4, Na_2HPO_4, Na_3PO_4 and $Na_2C_2O_4$ were obtained from Tianjin Tianli Chemical Reagent Co., LTD. (Tianjin, China). $Na_3C_6H_5O_7$ and $Na_2C_{10}H_{16}N_2O_8$ (EDTANa_2) were obtained from Tianjin Shen'ao Chemical Reagent Co., LTD. (Tianjin, China). $Cd(NO_3)_2$ was obtained from Chengdu Kelong Chemical Reagent Company (Chengdu, China). $Mn(NO_3)_2$ was obtained from Tianjin Guangfu Technology Development Co., Ltd. (Tianjin, China). $Pb(NO_3)_2$ was obtained from Tianjin Guangfu Fine Chemical Research Institute (Tianjin, China). $Cr(NO_3)_3$, oleic acid and diethylene glycol (DEG) were obtained from Tianjin Fuchen Chemical Reagents Factory (Tianjin, China). Ammonia, ethanolamine, N,N-dimethylformamide (DMF), ethylene glycol (EG) and hydrazine (N_2H_4) were obtained from Fuyu Chemical (Tianjin, China). Toluene and chloroform were obtained from Tianjin Yongsheng Chemical Reagent Co., LTD. (Tianjin, China). Mineral oil was obtained from Sigma-Aldrich (Shanghai, China). Dichloromethane was obtained from Sinopharm Chemical Reagent Co., LTD. (Shanghai, China). All the above chemicals and reagents were used without further purification. All the solutions used in the study were prepared by ultrapure water (> 18.2 MΩ cm) from Milli-Q Integral Water Purification System (Millipore, MA, USA).

2.2. Fabrication of paper-based capacitive sensors (PCSs) and their working principle

The bulk capacitive sensor was assembled by stacking filter paper and aluminum foil *via* double-sided tape (Fig. 1(1–3)). It was then tailored into 55 mm-long strips using No. 8014 paper trimmer (Deli Stationery, Ningbo, China). Finally, the as-tailored strips were further cut into 10 mm-width strips using Matrix™ 2360 programmable shear (Kinematic Automation Inc., CA, USA). Alternative geometries of PCSs can be easily prepared by adjustment of the length and width. The non-sticky covering film of the double-sided tape remained to attach on both sides of the sample-loading region. All the PCSs were kept in dry status prior to use.

PCSs consist of three areas, including the loading area, spacer area and capacitance area (Supplementary Fig. S1a). After the analyte is loaded, it flows through the filter paper due to the capillary action and wick the capacitance area (Fig. 1(4)/(5)). Here, the analyte can be either homogenous (e.g., pure organic chemical liquids) or heterogeneous (e.g., heavy metal salt solutions). For some heterogeneous solutions, for example, heavy metal salt solutions, if the solvent (i.e., water) is evaporated completely, the solute will be left (Fig. 1(6)).

According to the working principle of the developed PCSs (see details in Appendix A), the capacitance of the developed PCSs (C_P) is related to the dielectric constant (ε_r) of the analyzed sample. The dielectric constant, the ratio of permittivity between a substance and free space, depends on molecular properties (e.g., polarity, interactions
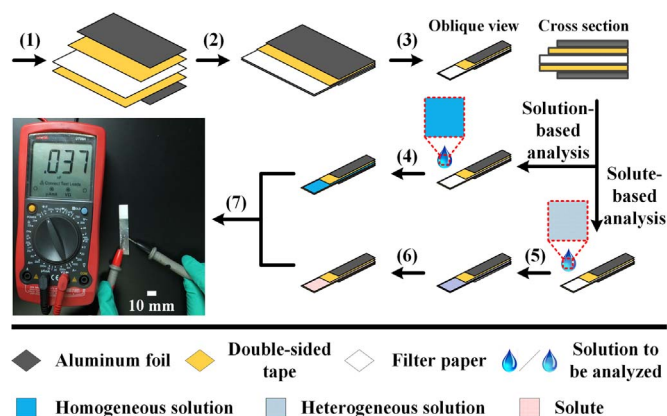
Fig. 1. Schematic of the preparation and application of paper-based capacitive sensors (PCSs). (1) Tailor the components of PCSs, *i.e.*, aluminum foil, double-sided tape, and filter paper into designated shapes; (2) Stack the components orderly layer by layer through double-sided tape; (3) Cut the as-assembled bulk into individual sensors. For solution-based analysis, just load the solution to be analyzed and wait it to wet through the sensor (4), while for solute-based analysis, perform a similar operation (5), and then wait the solvent to evaporate completely (6). Finally, employ a handheld multimeter for capacitance measurement (7).

with neighbouring molecules [38]) and also the frequency of the applied alternating current (AC) electric field. Thus, as ε_r varies with different kinds of substances [39] and their concentrations [40], the measured C_p varies correspondingly and so can be used for identification and quantification of chemicals. Meanwhile, from the electric field, and its molecules deviate so as to oppose the characterization of the dielectric properties of double-sided tape and filter paper, it is found that the ε_r and dielectric loss (tan δ) vary with frequency (Supplementary Fig. S2e–f). When AC electric field is applied, the dielectric material between the electrodes is polarized by the effect of the oscillating vector of applied field. At a microscale, the frequency of oscillating current affects the ability of the molecules to deviate from their original state towards the electrodes along the direction of applied field. As higher frequency is applied, the molecules cannot "catch up" before the direction of the field changes again, thus showing a decreased level of deviation from its original state. This immobility at high frequency causes a diminished reaction towards the field, its dielectric relaxation, and dielectric constant, thus reducing the capacitance. At low frequency, however, the molecules oscillate with the applied field, which corresponds to their physical and chemical properties. This distinguishing ability enables the usage of easily available multimeter (~400 Hz, a low frequency) as an alternative instrument for direct measurement to other expensive and professional dependent equipment, which as well suits the POCT requirements (Fig. 1(7)). Meanwhile, capacitance varies with frequency, and thus frequency spectrums of capacitance are expected to manifest even more detailed information related to the analyte. Additionally, dielectric loss, quantifying the inherent capability of dielectric materials to dissipate electromagnetic energy (*e.g.*, as heat), also depends on type and amount of the dielectric materials. The dielectric property is related to both real and imaginary components of the dielectric constant, and can be parameterized in terms of loss tangent (tanδ), which thus can also be used for chemical identification and quantification.

2.3. Measurement of dielectric performances

PCS was laid on a flat and clean surface. Sample was added to the loading area of the sensor using a micropipette and it was wicked to the capacitive area. Measurement of dielectric performances was carried out using a UT58 multimeter (UNI-T, Dongguan, China) or Agilent E4982A LCR meter (Agilent Technologies Inc., CA, USA) with AC of 1 V peak voltage and frequency range of 100 Hz - 1 MHz.

2.4. Statistical analyses

To adapt multivariate chemometrics strategies for numerical analyses can minimize instrumental noises and interferences, and then bring significant improvement for identification and determination of chemicals. However, such numerical analyses usually rely on extra and professional operations, which is not suitable for rapid tests applications at the point of care. We thus chose the most common-used average values for data analyses in this study. Student's *t*-test was used to analyse the differences between two separated measurements. $p < 0.05$ means significant difference, while $p > 0.05$ means no significant difference.

3. Results and discussion

3.1. Exploration of the effects of structures of the developed PCSs on their performance

Based on the calculated equation of capacitance, the capacitance of a parallel-plate capacitor is dependent on the area and distance between the electrode plates. For the developed PCSs, the distance between the electrode plates is kept constant (*i.e.*, the total thickness of the paper and double-sided tape layers). The area of the electrode plate (capacitance area) is then the main affecting factor. However, for the PCSs with the same area but different W_c/L_c ratios, these PCSs may have some differences in solution flow and distribution. To check the effect of W_c/L_c ratio on their performance, we designed PCSs with different conformations (altered width and length), but with the same capacitance area (Fig. 2a). We loaded 70 μL of ultrapure water and measured the capacitance at a frequency of 1000 Hz in ambient condition (Fig. 2b). We found that the values of measured capacitance (C_p) first increased; and subsequently, C_p values of #1−3 PCSs were almost stable, while C_p values of #4−7 PCSs decreased with time. Furthermore, with a wider width and a shorter length, the maximum capacitance can be reached in a shorter time.

According to our previous study [41], for the capillary flow in filter paper, the wicking liquid front height can be theoretically calculated using Lucas−Washburn equation:

$$h = \sqrt{\frac{4\sigma\cos\theta}{\mu}\frac{K}{\varepsilon R}} \cdot t^{1/2} \tag{1}$$

The corresponding liquid speed can then be defined as:

$$S = \frac{dh}{dt} = \sqrt{\frac{\sigma\cos\theta}{\mu}\frac{K}{\varepsilon R}} \cdot t^{-1/2} \tag{2}$$

In Eqs. (1) and (2), h, S, σ, μ, θ, K, R, t are theoretical wicking liquid front height, theoretical liquid speed, interfacial tension, viscous, contact angle, permeability, effective pore radius, and time, respectively. For the same solution and filter paper, it can be regarded as $h \propto t^{1/2}$ and $S \propto t^{-1/2}$. Further, our previous study revealed that the width has no significant effect on the wicking height when the wide end of filter paper is fully in contact with water. Therefore, for #1−3 PCSs, the PCS with a shorter length takes a shorter time to wet the capacitance area and consumes the loading solution faster, since water mainly flows along the direction of length (unidirectional). For #4−7 PCSs, the capacitance area absorbed water both along the direction of length and width (bidirectional). We thus hypothesized that the PCSs with either larger length or larger width would obtain a relatively smaller water distribution area compared to the others after the same time lapse. Meanwhile, the slower water is wicking, the larger amount of water is lost due to evaporation. As a whole, although the capacitance areas of all the PCSs were kept the same, the value of C_p and its variation curve are not the same. As W_c increased, the measured capacitance increased first and then decreased. In comparison, #3 PCS (W_c/L_c=10 mm/ 40 mm) was chosen in the following experiments, since the measured
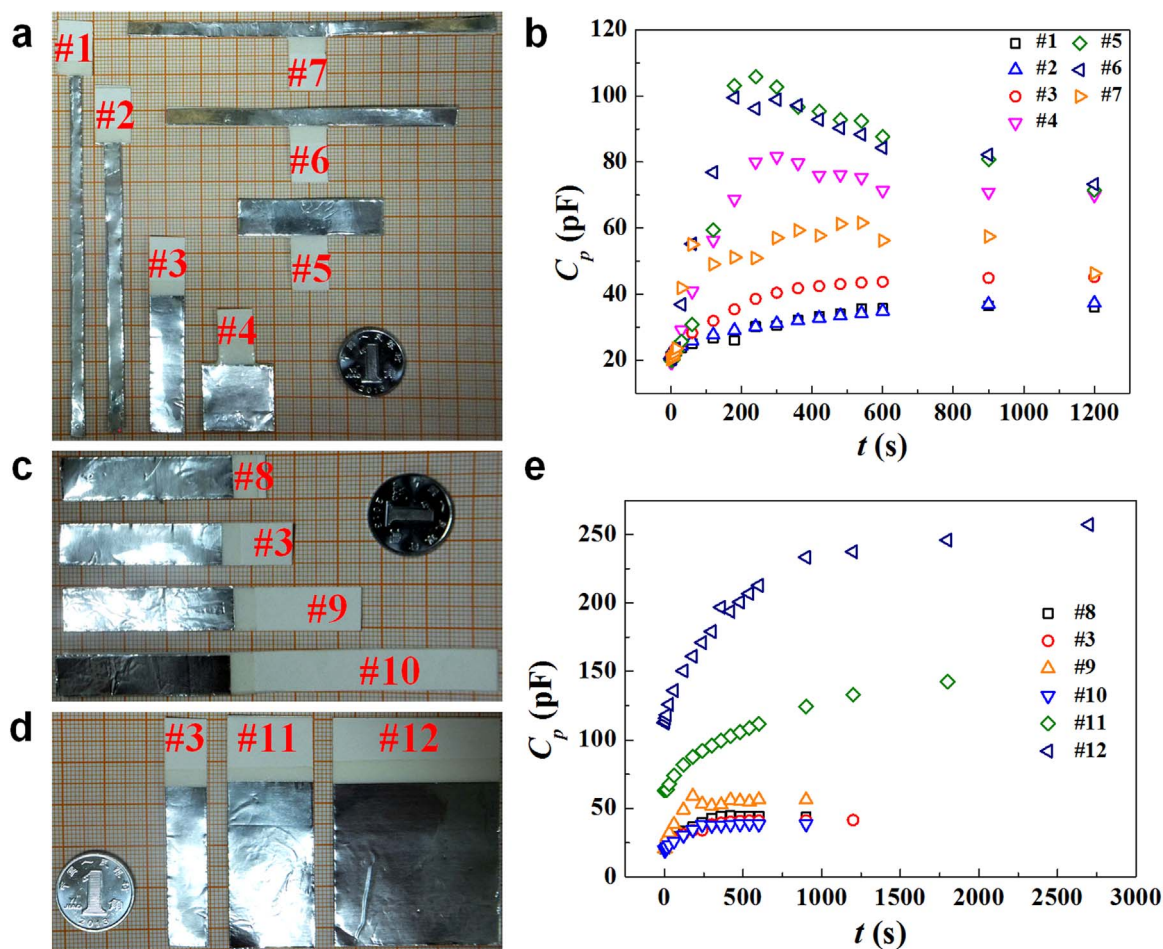
Fig. 2. The effect of geometry of PCSs on their performances, including W_c/L_c ratios, loading area, and capacitance area. (a) Images of #1-#7 PCSs that have the same A_c as well as loading and spacer areas but different W_c/L_c ratios. (b) Changes of measured C_p with time after sample is loaded on the PCS. (c–d) Images of #8-#12 PCSs with #3 PCS as a reference, in which (c) is for #8, #3, #9, and #10 with increasing loading area but spacer and capacitance areas remain the same, and (d) is for #3, #11, and #12 PCSs with increasing area for the whole sensor as the width doubles while the length remains constant. (e) Changes of measured C_p with time after sample is loaded on the PCS. All the samples used are ultrapure water; for each PCS, the loading volume is proportional to the area of the whole filter paper, *i.e.*, 70 μL/550 mm². C_p: capacitance; t: time. Supplementary Table S1 gives values for dimensions W_c, L_c, L_l, W_l and A_c of #1-#12 PCSs, respectively.

result was relatively stable and higher.

To investigate the effect of the loading area and capacitance area on the performance of PCSs, we made two sets of PCSs, one set with different length (L_l) of loading area (including 2.5 mm, 10 mm, 25 mm, and 55 mm, Fig. 2c) and the other set with an increasing capacitance area (A_c, including 400 mm², 800 mm², and 1600 mm², Fig. 2d) respectively. We measured capacitance at a frequency of 1000 Hz under ambient conditions and found that the change of loading area (L_l) had a limited effect on the variation of capacitance (Fig. 2e). #9 PCS expressed a little higher capacitance, while #8 and #10 PCSs showed a similar C_p-t relationship with #3 PCS.

To assess the effect of A_c, we increased the area by increasing the overall width of the fabricated PCSs while keeping the length the same. We found that the capacitance proportionally increased with increasing capacitance area (A_c), *i.e.*, C_p increased about two times as Ac doubled (Fig. 2e). The reason is quite straightforward; according to Eq. (8) in Appendix A, the capacitance increases proportionally with the area of the electrode plates. However, the time taken to achieve a stable measurement and usage amount of sample increased as A_c increased [42,43]. If a smaller sensor is used, less fluid sample is needed to be loaded and less time taken for the capacitance to achieve a stable value. Therefore, #3 PCS was chosen for the following experiments. To further explore the stability of PCSs during manufacturing, we prepared 7 batches of #3 PCSs in different time, made them dry using an oven, and then measured their capacitances, respectively

(Supplementary Fig. S3). The measured value was 23.0 ± 0.3 (95% CI), which did not vary significantly. The manufactured PCSs are thus supposed to own a good reproducibility.

3.2. Study on the factors relevant to the usage of the developed PCSs

To investigate the effect of loading volume and to compare the accuracy of a multimeter to a LCR meter, we measured the capacitance of #3 PCS loaded with a serial volume of 1 mM $NaNO_3$ using multimeter and LCR meter. According to the manufacturer's instructions, the frequency of the multimeter is about 400 Hz. We thus chose the measured results at 400 Hz (exactly 398.107 Hz) and 1000 Hz using LCR as reference (Fig. 3a). For the solution-based analysis, we found the capacitance signals increased by almost 100% when the loaded volume increased from 10 μL to 60 μL; between 0 and 10 μL, the signals had smaller (for multimeter-based) or insignificant differences (for LCR-based), while the signals almost reached a plateau when the volume was greater than 60 μL. The overall pore volume of the PCS can be computed with the equation:

$$V_{pore} = V_p \eta \tag{3}$$

where V_p is the total volume of filter paper ($V_p = A_p \times d_p = 5.5 \times 10^{-4}$ m² $\times 1.8 \times 10^{-4}$ m) and η is the effective porosity of paper (0.57) (Supplementary Table S2). Thus, $V_{pore} = 56.43$ μL, which is just 6% smaller than the measured value (60 μL). Meanwhile, a larger
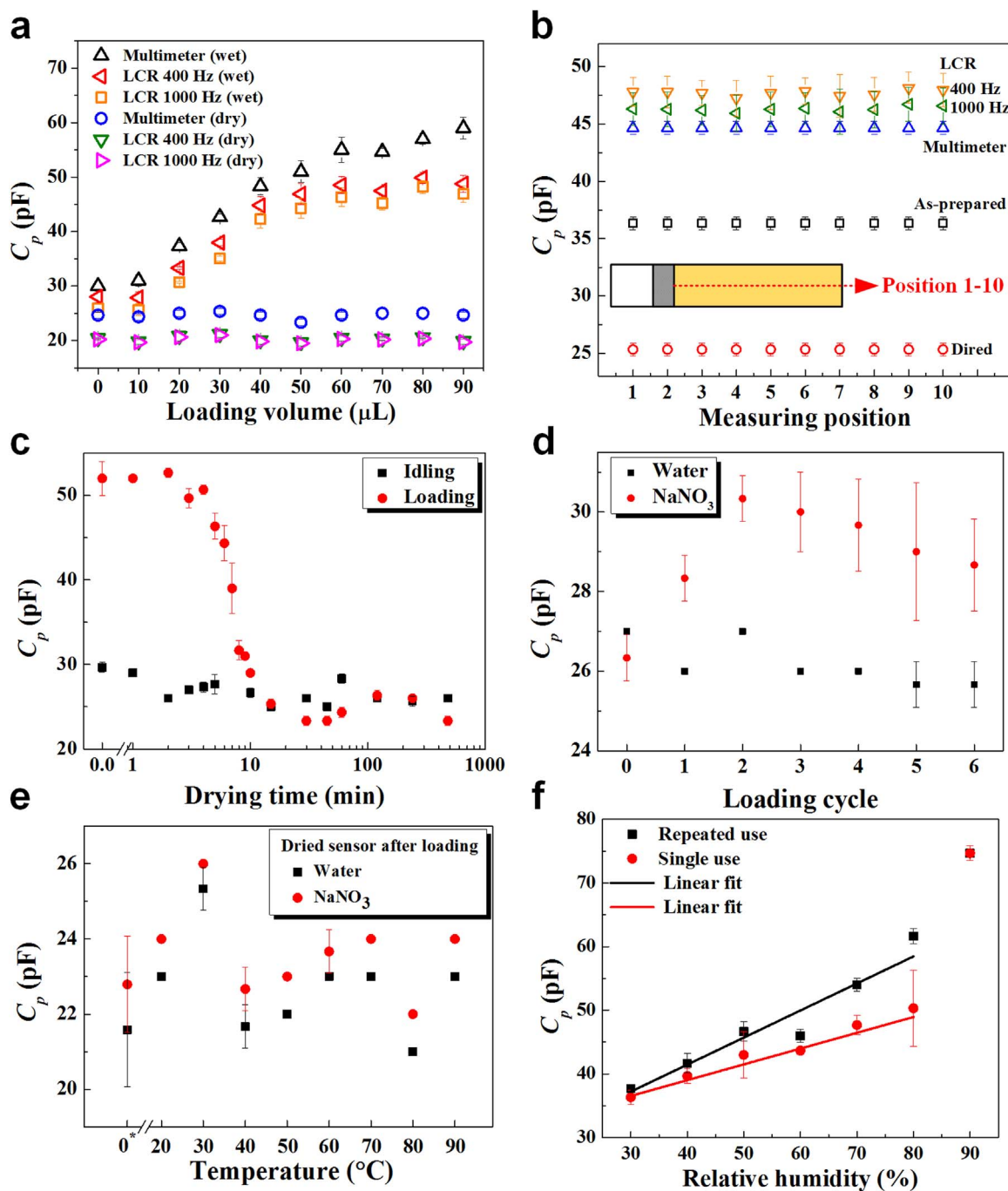
Fig. 3. The effects of some important parameters on the performance of #3 PCS. (a) Loading volume, measurement instrument and measurement status (wet or dry) (*n*=3). (b) Electrode position on the PCS for capacitance measurement (*n*=3). (c) For dry status measurement, exploration of the drying time (*n*=3). (d) The effect of loading cycle for dry status measurement. A cycle means the whole procedure of loading and drying of samples. The effect of temperature (e) and relative humidity (f) for dry status measurement. In (e), 0* is pointed to room temperature (temperature: 20 ℃, relative humidity: 30%, *n*=24), for the others, *n*=3. For (b) and (c), the sample loaded is 1 mM of $NaNO_3$, and for (d) and (e), the concentration of $NaNO_3$ is 1 mM and 1 M, respectively. For (a, c-e), the volume of loading sample is 70 μL.

volume of solution (> 70 μL) stayed at the loading area of the PCS up to 5 min for solution flow and distribution. Further increase of solution volume (> 90 μL) resulted in overflowing. Thus, to let the filter paper saturate with the sample, a 70 μL loading volume was chosen for the following experiments, considering the time cost and sample consumption. When the solution was dried completely (dry status measurement for solute-based analysis), the measured capacitance values showed no significant differences from diverse volumes (*p* > 0.05). This indicates that the difference during wet status measurement is mainly due to the existence of water. Drying water completely is thus expected to improve the accuracy for solute-based analyses. Further, we noticed that there is an

obvious difference of capacitance value for the idling PCS measured before and after drying (the data of 0 μL of loading volume). The reason may be that PCSs, especially the filter paper part, contain some amount of moisture prior to use due to storage in ambient conditions (Supplementary Fig. S4). Therefore, it is important to consider storage humidity and whether drying should take place prior to use. However, overall, while the absolute value measured may be different with moisture level, they shared the same variation trend *i.e.*, multimeter > LCR 400 Hz > LCR 1000 Hz, indicating that the multimeter is a good candidate for measurement of capacitance. Therefore, the multimeter was mainly chosen for the following capacitance measurements.
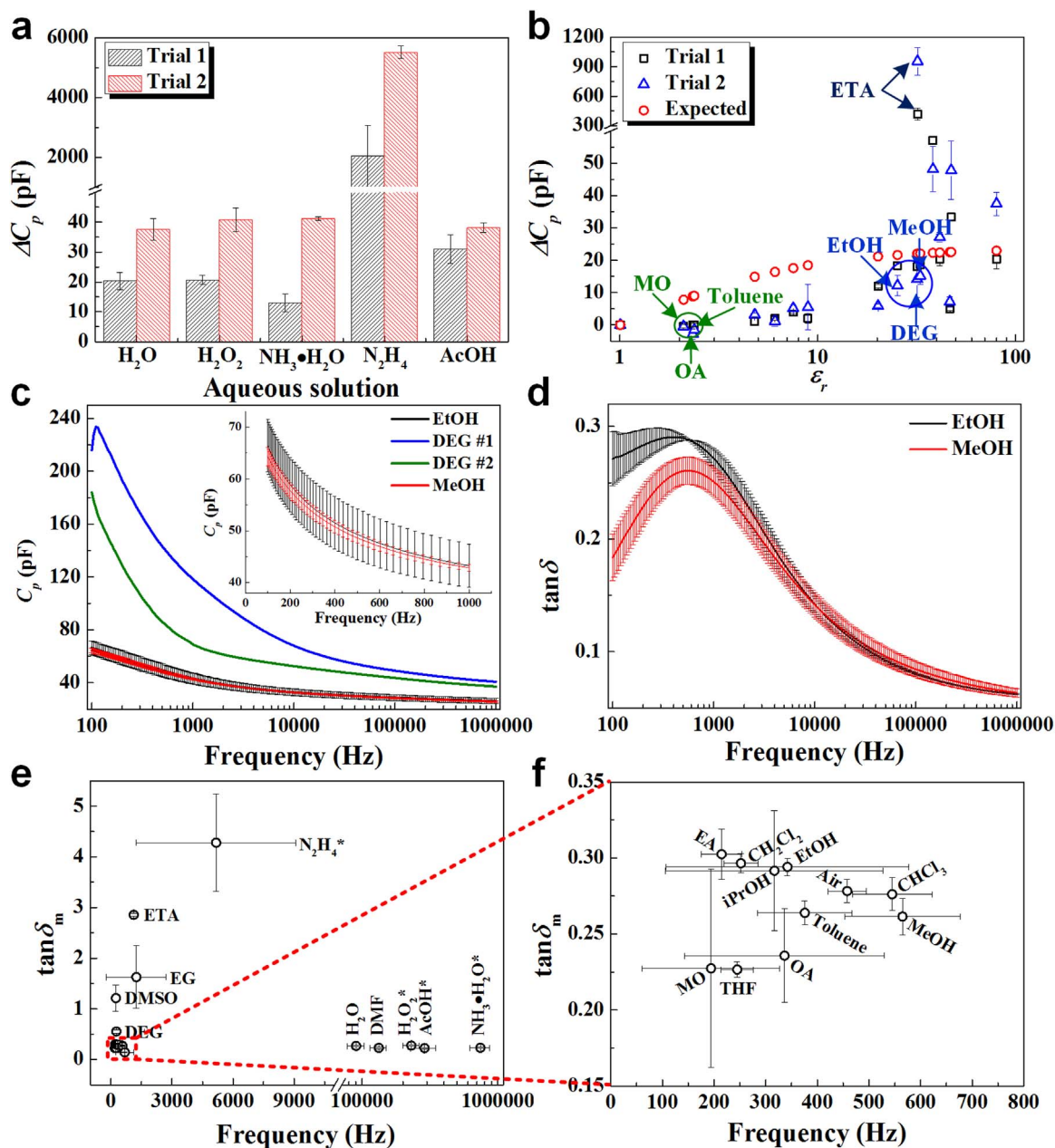
Fig. 4. Identification of liquids. (a) The measured capacitance value of concentrated aqueous solution using dried (trial 1) and as-prepared (trial 2) PCSs. (b) The measured capacitance value changes with dielectric constant using dried (trial 1) and as-prepared (trial 2) PCSs as compared to theoretically prediction. (c) The capacitance value changes with frequency for EtOH, DEG, and MeOH, respectively. (d) The dielectric loss ($\tan\delta$) changes with frequency for EtOH and MeOH, respectively. (e) The maximum dielectric loss ($\tan\delta_m$) for each fluid at its peak value in the dielectric loss ($\tan\delta$) – frequency spectrum and (f) is the plot for the substances that exist in smaller frequency range in (e).

To explore the effect of the electrode position on the performance of PCSs, we measured the capacitance of #3 PCS in 10 different positions at 4 mm intervals in three situations, *i.e.*, as-prepared, dried and sample loading, respectively (Fig. 3b). We found that the capacitance values are close to be stable. One-way ANOVA indicated that the position of the electrode had no significant effect on the results ($p > 0.05$), which agrees well with the working principle of the parallel-plate capacitor. We also found that the capacitance values of as-prepared PCSs were higher than that of the dried ones. Since we first measured the capacitance using multimeter and then LCR meter after 70 μL of water was loaded, the multimeter-measured values were a little lower but still higher than that of as-prepared PCSs. We speculate that the analyte had not yet fully wetted the paper during measurement by multimeter. Making PCSs dried increases their sensitivity to water content. The results demonstrated that the multimeter accurately

measured the capacitance.

For solute-based analyses, the solute flowed and distributed as the solvent flowed and distributed. To remove the effect of water-solvent due to its high dielectric constant, we measured the capacitance of an unloaded PCS (idling) and a PCS loaded with 70 μL of water (loading) as time lapses while drying (Fig. 3c). The capacitance became stable after 10 min of drying. As a result, 15 min was used in the drying process for solute-based analyses. For dry status measurement, we further studied the effect of increased salt amount on the capacitance through multiple times of loading and drying the solution into the PCS (Fig. 3d). We found that the capacitance value increased and then decreased as the loading cycles of salt solution increased. However, this phenomenon happened to the PCS with water loading as well. The capacitance difference between loading salt and water reached to the maximum at the 3rd loading cycle, while the capacitance value for salt

analyses reached to the maximum at the 2nd loading cycle. This phenomenon indicated that although multiple loading of sample increased the amount of solute for analysis, the repeated cycles may affect the properties of the PCS as well. Moreover, the deviation of the capacitance measurements was much bigger in detection of salt solution, which may be a result of interferences from the salt. When the loading cycle increases, the deviation of capacitance of water increases as well. Such big deviation should be due to the performance of the PCS affected by the repeatedly loading and drying of samples. We suspect that the repeated heating may change the properties of chemicals on the double-sided tape and deform the shape of the filter paper. However, the even more detailed or exact reasons may require further exploration. Therefore, the loading cycle is better not more than three times, which can avoid the big deviation in detection. Since the PCS is low-cost and disposable, the PCSs were mainly designed for one sample loading cycle for solute-based analysis, and requires much more explorations for detection of clinical sample.

Finally, temperature and relative humidity as controlling factors of the dielectric constant of paper have been discussed earlier [44–47]. Here, we briefly explored their effects on the performance of PCS (Fig. 3e). As temperature increased, we observed variations in the measured capacitance. However, the value of the PCS with NaNO$_3$ loading was always higher than that of the PCS with water loading. The average value at different temperatures showed no significant difference compared to the value measured at ambient condition for both analyses of water and salt (paired t-test, $p > 0.05$, $n=3$). It indicates that PCS are appropriate for use at temperatures ranging from 20 °C to 90 °C. Further, we measured the capacitance of PCSs using the same sensor (*i.e.*, each relative humidity consumes one individual sensor three times) and different sensors (*i.e.*, each relative humidity consumes three different sensors one time) with the multimeter in a hygro thermostatic chamber with a gradient relative humidity (from 30% to 90%) at 25 °C without loading any fluid. The capacitance increases with increasing relative humidity. It is found that using the same sensor showed higher relative humidity sensitivity than using different ones. From 30% to 80% relative humidity, the capacitance increased linearly ($R^2=0.933$ for repeated use and $R^2=0.964$ for single use, respectively), while the capacitance increased greatly from 80% to 90%. This indicates that a higher relative humidity enabled PCS to absorb a higher volume of water. For 90% relative humidity, however, the relative humidity was too high and was roughly similar direct water loading on the PCS.

3.3. Identification of chemicals

In theory, chemical identification is expected to be realized through the difference between the dielectric constants of the sample loaded into the PCS, which is further expressed as the measured capacitance (C_p). Meanwhile, according to the aforementioned studies, the PCSs, dried or not, show great differences in the values of measured capacitance. In practical applications, the PCSs are easily wetted. To study the PCSs for chemical identification under different situations, we performed this study using dried (trial 1) and as-prepared (trial 2) PCSs. We loaded several different aqueous solutions and organic liquids into PCSs and measured their capacitance (C_p) using multi-meter first (Supplementary Table S3, Fig. 4a–b). In Fig. 4a, we found the measured value was higher in trial 2 than that in trial 1. However, hydrazine aqueous solution posed an extremely higher capacitance value in both two trials. For the other three kinds of aqueous solutions, the measured capacitance showed no significant differences compared to pure water in the trial 2 (Student's t-test, $p > 0.05$, $n=3$), while in the trial 1, the measured capacitance of ammonia and acetic acid solution showed distinguishable differences. It is demonstrated that for identification of aqueous solution, it is better to perform using dried PCSs, in order to reduce the effects of water. In Fig. 4b, the measured capacitance was presented as their dielectric constants. Similarly, the

value in the trial 2 is higher than that in the trial 1. Except several chemicals induced a relatively higher capacitance, especially ethanolamine, the capacitance of the remaining chemicals increased with increasing dielectric constant, which agrees with the theoretical expectation.

Although it provides a certain accuracy to identify some chemicals, however, the measured capacitance is limited to distinguish all the chemicals, for example ethanol (EtOH), DEG, and methanol (MeOH) in trial 2. We thus further measured their frequency spectrum of capacitance (C_p) and dielectric loss (tanδ) using an LCR meter (Fig. 4c–d, all the measured frequency spectra of capacitance are shown in Supplementary Fig. S5). Compared with trial 2, trial 1 provides a relatively higher selectivity to identify all the chemicals. In trial 1, it is difficult to distinguish between CHCl$_3$ and CH$_2$Cl$_2$, and MO and OA (Fig. S5a). On the contrary, it is very easy to identify hydrazine, ethanolamine, DEG, EG, DMF, DMSO and glycerol in comparison to the other measured chemicals using the frequency spectrum of capacitance in trial 2 (Supplementary Fig. S5d). However, for other aqueous solutions (Supplementary Fig. S5e) or organic chemicals (Supplementary Fig. S5f), it is limited to identify them with enough accuracy. Taken EtOH, DEG and MeOH as an example for a detailed explanation (Fig. 4c), both two capacitance—frequency spectrum curves of DEG are significantly different from those of both MeOH and EtOH. The capacitance—frequency spectrum curves of MeOH and EtOH almost overlap. The inset in Fig. 4c further clearly demonstrated it is not easy to identify MeOH and EtOH. It is found that a great difference exists between the two capacitance—frequency spectrum curves of DEG, illustrating a poor repeatability for the frequency spectrum analysis. This problem may need further studies. Here, for the further identification of MeOH and EtOH, we analyzed their dielectric loss—frequency spectrum (Fig. 4d). We find that as frequency increases, dielectric loss tanδ of both MeOH and EtOH first increases and then decreases, while the maximum tanδ (tanδ_m) and corresponding frequency of these two chemicals are different. Therefore, it is easier to tell from MeOH and EtOH using dielectric loss—frequency spectrum. Subsequently, we analyzed all the dielectric loss—frequency spectrum of the chemicals and found the tanδ_m and its corresponding frequency for each chemical (Fig. 4e). Those chemicals with distinguishable capacitance—frequency spectrum are shown different tanδ_m—frequency values (Fig. 4e). Meanwhile, all the aqueous solutions are easily identified as well. Fig. 4f is further shown a clear result for the remaining chemicals. Since the LCR meter provided the frequency by an exponent increase instead of a linear increase, the accuracy is affected. However, for the identification of chemicals with similar structures, such as MeOH and EtOH, CH$_3$Cl and CH$_2$Cl$_2$, and so on, the tanδ_m—frequency works well.

3.4. Quantification of chemicals

To explore the capability of quantification using the developed PCS, we employed PCSs for analyses of solvent mixtures and electrolyte solutions, respectively. Considering water has a higher dielectric constant, if it mixes in a chemical, especially those chemicals with a lower dielectric constant, the resulting dielectric constant may be greatly different; or vice versa. According to this analysis, the developed PCSs are expected to not only identify (Fig. 4a) but also quantify the concentration of the mixture solution. First, taking ethanol (ε_r=25.3) – water (ε_r=80.1) mixture as an example, the measured data of as-prepared PCSs showed a higher capacitance values than that of dried PCSs, but they shared the same variation trend, *i.e.*, increased as the volume of ethanol decreased (or the dielectric constant increased) (Supplementary Fig. S6). Using a volume fraction of ethanol increasing from 30% to 100%, the change of measured capacitance shows a linear relationship. After the volume fraction falls below 30%, the LCR meter-based data showed no significant difference, while for multimeter-based data, it kept increasing, although with a decreasing amplitude. It
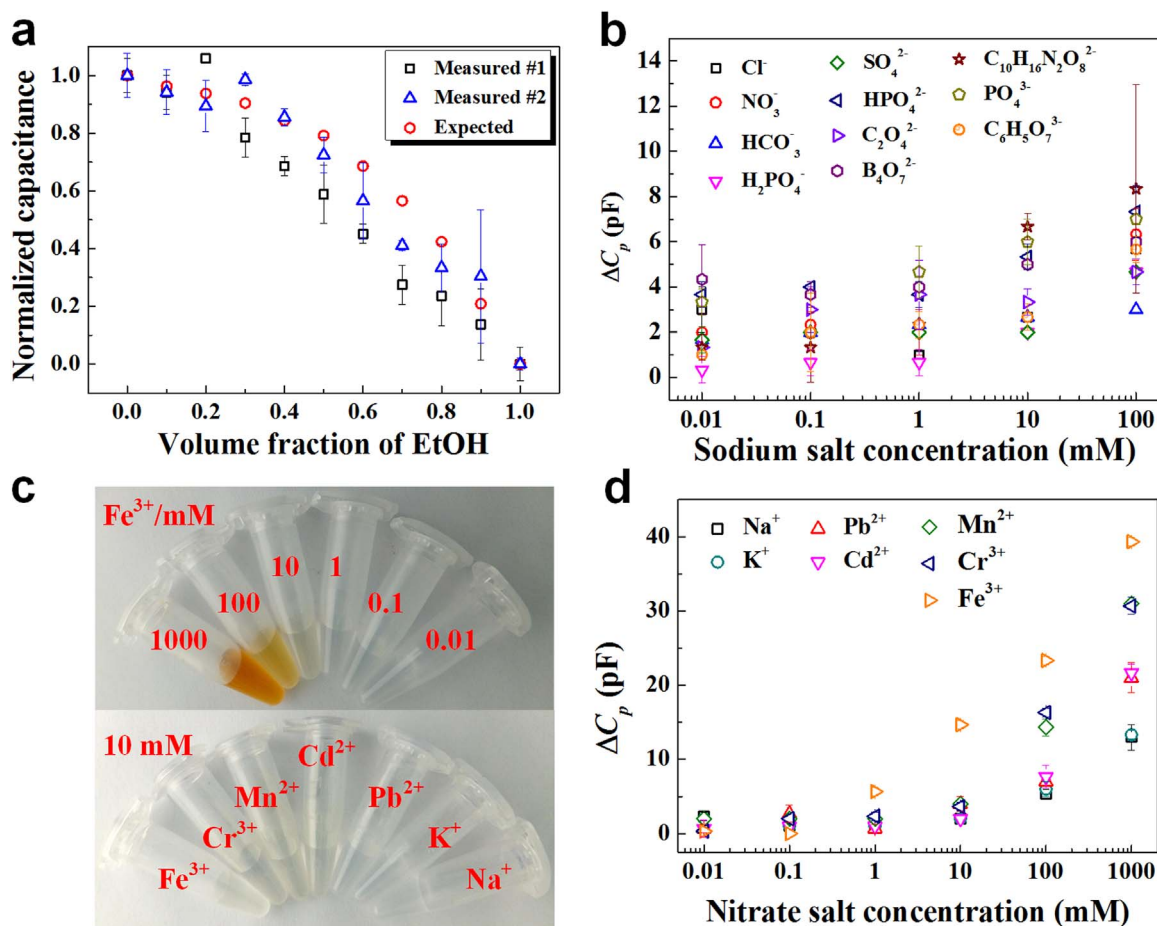
Fig. 5. Quantification of solution concentrations. (a) The normalized capacitance changes with volume fraction of ethanol in ethanol-water mixture. (b) The capacitance changes with concentrations of various sodium salts after drying. (c) The images of Fe^{3+} with different concentrations and 10 mM of different nitrate salts. (d) The capacitance changes with nitrate salt concentration after drying.

is further demonstrated here that the multimeter showed a comparable quantification accuracy compared to LCR meter. However, the difference in theoretical capacitance values between EtOH and H_2O is smaller than the measured values, which may be contributed to the differences in their mobility in filter paper and evaporation to the environment. Under the normalized capacitance, it is found that the measured results basically agree with the expected ones, either for the as-prepared PCSs or for the dried ones (Fig. 5a).

Subsequently, we explored the application of the PCS for the quantification of concentrations of ions, especially heavy metal ions, in water. First, we prepared a series of concentrations of sodium salts for study of the effects of anions. As shown in Fig. 5b, the measured capacitance generally increased as the concentration increased. For different anions, the variation trends are not totally the same and, the limit of detection (LOD) is correspondingly different. In a word, although it is difficult to identify the exact anion, quantifying the concentration of one or more anions using capacitance value measured by multimeter has been proven to work. Next, we used a similar strategy to quantify the concentration of heavy metal ions. We measured the capacitance of several nitrate salt samples with a gradient concentration (Fig. 5c–d). As differences in capacitance presented by the salt are induced by the varying dielectric properties, they are in fact affected by the polarization effect on the ionic bonding between the ions in the salt crystal [48–50]. This ionic bond strength is determined by the ions' charge (valency) and their ionic sizes, which also contributes to the lattice energy of the salt. Smaller ionic sizes and greater charges contribute higher lattice energy. The order of the nitrate salts, having largest to smallest capacitance at concentration of

1 M, *i.e.*, $Fe^{3+} > Cr^{3+} > Mn^{2+} > Cd^{2+} > Pb^{2+} > Na^+ > K^+$ is comparable to the order of their charge (trivalent to monovalent) and ionic size (smallest to largest). At a low frequency (~400 Hz), ionic molecule has long relaxation time, allowing it to react during the oscillating electric field takes place. Our sensor could not differentiate among monovalent ions, *i.e.*, Na^+ and K^+, indicating its functionality to detect ions with higher charge. In a word, the PCS could sense the concentration of Fe^{3+} as low as 1 mM (Fig. 5d), which is more sensitive than the naked eye's observation (Fig. 5c). For a lower concentration of metal ions, *i.e.*, 10 μM, the sensor can sense them but further exact differentiation may need the help of an LCR meter for capacitance spectrum or dielectric loss analyses.

Considering the Criterion Continuous Concentration (an estimate of the highest concentration of material in surface water that can be exposed by an aquatic community indefinitely without suffering from an unacceptable effect) of Fe recommended by the United States Environmental Protection Agency (EPA) is 18 μM (https://www.epa.gov/wqc/national-recommended-water-quality-criteria-aquatic-life-criteria-table), the proposed method still suffers lack of selectivity as well as sensitivity to meet the requirements for water quality analysis for human health and safety at point of care (POC). However, these techniques for water quality analysis involve trade-offs of cost, ease of use, and performances. For example, atomic absorption spectrometry and inductively-coupled plasma mass spectrometry offer high sensitivity and selectivity at the expense of cost and ease of use, and require professional staff to perform such measurements in standard laboratories. Therefore, the significance of this study is to provide alternative concept for chemical identification and quantification and

further demonstrate its potential applications in water quality analysis. Compared with centralized laboratory technologies, the proposed one is very suitable to perform in resource-limited settings since it is general, simple, and low-cost. Actually, users of technology want technology to be useful as well as simple and cheap [51]. Various similar concepts has been reported, for example, using magnetic levitation to characterize samples of food and water based on measurements of density [52]. These technologies have their drawbacks but they own great potentials to bring effective contributions to chemical analysis.

4. Conclusion

Here, we have developed a PCS and demonstrated it to be a versatile tool for identification of chemicals using dielectric properties, including capacitance value, dielectric loss and frequency spectrum. The optimized PCS (10 mm of width and 55 mm of length in overall) only takes about $0.01 to prepare and uses 70 µL of solution (either pure chemicals or aqueous mixtures) for analysis. For the same PCS containing an organic chemical to be analyzed, end-users can measure its signals using hand-held multimeter (for capacitance measurement) or LCR meter (for frequency spectrum of capacitance and dielectric loss measurement simultaneously) for chemical identification, which is simple and rapid. To further improve the PCSs and establish a database of dielectric properties, such as frequency and temperature spectrum of standards for references, it will serve as an alternative way for identification of organic chemicals.

Additionally, the method reported here works well for chemical quantification. Considering the conditions in resource-limited settings and the requirements of POCT, we measured the signals using multimeter and found this method could quantify both the volume fraction of ethanol in ethanol-water mixtures and the molar concentration of salt solutions. The method does not require complicated design and fabrication procedures, or refined chemical preparation and modification. The whole procedure is as simple and rapid as the one for chemical identification. For heavy metal ion detection, however, the LOD of PCSs does not yet achieve the criteria set by authorized bodies, *e.g.* the United States Environmental Protection Agency (EPA) and the World Health Organization (WHO). Nevertheless, qualitative determination of chemicals could be made possible by referring to an increase or decrease of capacitance compared to that of a pure substance. Therefore, this sensor can serve as a fast qualitative determination tool, which acts an example for POC application.

In summary, this study reported the fundamentals of PCSs and demonstrated versatility and feasibility of applications of such sensors. As a proof of concept, we chose diverse kinds of chemicals ranging from organic solutions to heavy metals salts to assess performances of the proposed method. Compared with standard laboratory based methods, however, the proposed one is current lack in sensitivity and selectivity, and thus is too difficult to determine chemical compounds in real samples at desired concentration ranges, which requires further study to improve its performances. Following this strategy, our next study is intended to optimize the design of PCSs by replacing aluminum foil and double-sided tape using copper conductive tape and introducing specific sensing molecules using chemical modification. The modified one would improve sensitivity and selectivity, but they would increase cost and complexity as well. On the contrary, considering paper is ubiquitous and environmental friendly, these PCSs are low-cost and easy-to-use, enable various chemicals detection at the point of care, and thus can be used as first responses for rapid chemicals screening We believe this low-cost and label-free method will provide a new reference in the biochemical analysis. To the best of our knowledge, this work is the first comprehensive study on the development and application of PCSs.

Declarations of interest

The authors declare that they have no competing interests.

Appendix A. Supporting material

Supplementary data associated with this article can be found in the online version at doi:10.1016/j.talanta.2016.12.086.

References

[1] R.M. Silverstein, F.X. Webster, D. Kiemle, D.L. Bryce, Spectrometric Identification of Organic Compounds, 8th Edition, John Wiley & Sons, Hoboken, New Jersey, 2014.
[2] D.T. Quang, J.S. Kim, Fluoro- and chromogenic chemodosimeters for heavy metal ion detection in solution and biospecimens, Chem. Rev. 110 (10) (2010) 6280–6301.
[3] E. Snow, F. Perkins, E. Houser, S. Badescu, T. Reinecke, Chemical detection with a single-walled carbon nanotube capacitor, Science 307 (5717) (2005) 1942–1945.
[4] L.H. Yuen, R.M. Franzini, S. Wang, P. Crisalli, V. Singh, W. Jiang, E.T. Kool, Pattern-based detection of toxic metals in surface water with DNA polyfluorophores, Angew. Chem. Int. Ed. 53 (21) (2014) 5361–5365.
[5] J.N. Bixler, M.T. Cone, B.H. Hokr, J.D. Mason, E. Figueroa, E.S. Fry, V.V. Yakovlev, M.O. Scully, Ultrasensitive detection of waste products in water using fluorescence emission cavity-enhanced spectroscopy, Proc. Natl. Acad. Sci. USA 111 (20) (2014) 7208–7211.
[6] WHO/UNICEF, Progress on sanitation and drinking water - 2015 update and MDG assessment, WHO/UNICEF Joint Monitoring Programme for Water Supply and Sanitation, New York, USA, 2015.
[7] The United Nations, The millennium development goals report 2015, the Statistics Division of the United Nations Department of Economic and Social Affairs, New York, 2015.
[8] O. Tokel, F. Inci, U. Demirci, Advances in plasmonic technologies for point of care applications, Chem. Rev. 114 (11) (2014) 5728–5752.
[9] S. Zeng, D. Baillargeat, H.-P. Ho, K.-T. Yong, Nanomaterials enhanced surface plasmon resonance for biological and chemical sensing applications, Chem. Soc. Rev. 43 (10) (2014) 3426–3452.
[10] J. Sun, Y. Xianyu, X. Jiang, Point-of-care biochemical assays using gold nanoparticle-implemented microfluidics, Chem. Soc. Rev. 43 (17) (2014) 6239–6253.
[11] J. Yao, M. Yang, Y. Duan, Chemistry, biology, and medicine of fluorescent nanomaterials and related systems: New insights into biosensing, bioimaging, genomics, diagnostics, and therapy, Chem. Rev. 114 (12) (2014) 6130–6178.
[12] J. Zhang, Y. Xiang, D.E. Novak, G.E. Hoganson, J. Zhu, Y. Lu, Using a personal glucose meter and alkaline phosphatase for Point-of-care quantification of Galactose-1-phosphate uridyltransferase in clinical galactosemia diagnosis, Chem. – Asian J. 10 (10) (2015) 2221–2227.
[13] J. Zhang, Y. Xiang, M. Wang, A. Basu, Y. Lu, Dose-dependent response of personal glucose meters to nicotinamide coenzymes: applications to point-of-care diagnostics of many non-glucose targets in a single step, Angew. Chem. Int. Ed. 55 (2) (2016) 732–736.
[14] C. Parolo, A. Merkoçi, Paper-based nanobiosensors for diagnostics, Chem. Soc. Rev. 42 (2) (2013) 450–457.
[15] A.K. Yetisen, M.S. Akram, C.R. Lowe, Paper-based microfluidic point-of-care diagnostic devices, Lab Chip 13 (12) (2013) 2210–2251.
[16] B. Liu, D. Du, X. Hua, X.-Y. Yu, Y. Lin, Paper-based electrochemical biosensors: from test strips to paper-based microfluidics, Electroanalysis 26 (6) (2014) 1214–1223.
[17] Z. Nie, C.A. Nijhuis, J. Gong, X. Chen, A. Kumachev, A.W. Martinez, M. Narovlyansky, G.M. Whitesides, Electrochemical sensing in paper-based microfluidic devices, Lab Chip 10 (4) (2010) 477–483.
[18] L. Feng, H. Li, L.-Y. Niu, Y.-S. Guan, C.-F. Duan, Y.-F. Guan, C.-H. Tung, Q.-Z. Yang, A fluorometric paper-based sensor array for the discrimination of heavy-metal ions, Talanta 108 (2013) 103–108.

[19] A.M. López_Marzo, J. Pons, D.A. Blake, A. Merkoçi, High sensitive gold-nano-particle based lateral flow Immunodevice for Cd 2+ detection in drinking waters, Biosens. Bioelectron. 47 (2013) 190–198.

[20] Z. Fang, J. Huang, P. Lie, Z. Xiao, C. Ouyang, Q. Wu, Y. Wu, G. Liu, L. Zeng, Lateral flow nucleic acid biosensor for Cu2+ detection in aqueous solution with high sensitivity and selectivity, Chem. Commun. 46 (47) (2010) 9043–9045.

[21] D. Mazumdar, J. Liu, G. Lu, J. Zhou, Y. Lu, Easy-to-use dipstick tests for detection of lead in paints using non-cross-linked gold nanoparticle–DNAzyme conjugates, Chem. Commun. 46 (9) (2010) 1416–1418.

[22] J.-W. Han, B. Kim, J. Li, M. Meyyappan, Carbon nanotube based humidity sensor on cellulose paper, J. Phys. Chem. C 116 (41) (2012) 22094–22097.

[23] G. Shuster, S. Baltianski, Y. Tsur, H. Haick, Utility of resistance and capacitance response in sensors based on monolayer-capped metal nanoparticles, J. Phys. Chem. Lett. 2 (15) (2011) 1912–1916.

[24] S. Patel, T. Mlsna, B. Fruhberger, E. Klaassen, S. Cemalovic, D. Baselt, Chemicapacitive microsensors for volatile organic compound detection, Sens. Actuators B: Chem. 96 (3) (2003) 541–553.

[25] D.R. Kauffman, A. Star, Carbon nanotube gas and vapor sensors, Angew. Chem. Int. Ed. 47 (35) (2008) 6550–6570.

[26] A. Qureshi, J.H. Niazi, S. Kallempudi, Y. Gurbuz, Label-free capacitive biosensor for sensitive detection of multiple biomarkers using gold interdigitated capacitor arrays, Biosens. Bioelectron. 25 (10) (2010) 2318–2323.

[27] Z. Altintas, S.S. Kallempudi, Y. Gurbuz, Gold nanoparticle modified capacitive sensor platform for multiple marker detection, Talanta 118 (2014) 270–276.

[28] B. Wongkittisuksa, C. Limsakul, P. Kanatharana, W. Limbut, P. Asawatreratanakul, S. Dawan, S. Loyprasert, P. Thavarungkul, Development and application of a real-time capacitive sensor, Biosens. Bioelectron. 26 (5) (2011) 2466–2472.

[29] J. Lehr, Fv.C.B. Fernandes, P.R. Bueno, J.J. Davis, Label-free capacitive diagnostics: exploiting local redox probe state occupancy, Anal. Chem. 86 (5) (2014) 2559–2564.

[30] S. Dawan, P. Kanatharana, B. Wongkittisuksa, W. Limbut, A. Numnuam, C. Limsakul, P. Thavarungkul, Label-free capacitive immunosensors for ultra-trace detection based on the increase of immobilized antibodies on silver nanoparticles, Anal. Chim. Acta 699 (2) (2011) 232–241.

[31] J.-W. Park, S.S. Kallempudi, J.H. Niazi, Y. Gurbuz, B.-S. Youn, M.B. Gu, Rapid and sensitive detection of Nampt (PBEF/visfatin) in human serum using an ssDNA aptamer-based capacitive biosensor, Biosens. Bioelectron. 38 (1) (2012) 233–238.

[32] H. Berney, J. West, E. Haefele, J. Alderman, W. Lane, J. Collins, A DNA diagnostic biosensor: development, characterisation and performance, Sens. Actuators B: Chem. 68 (1) (2000) 100–108.

[33] B.Y. Won, H.G. Park, A touchscreen as a biomolecule detection platform, Angew. Chem. 124 (3) (2012) 772–775.

[34] S. Shrestha, C.M. Yeung, C.E. Mills, J. Lewington, S.C. Tsang, Chemically immobilized single-stranded oligonucleotides on praseodymium oxide nanoparti-cles as an unlabeled DNA sensor probe using impedance, Angew. Chem. Int. Ed. 46 (21) (2007) 3855–3859.

[35] S. Park, J. Hong, S. Choi, H. Kim, W. Park, S. Han, J. Park, S. Lee, D. Kim, Y. Ahn, Detection of microorganisms using terahertz metamaterials, Sci. Rep. 4 (2014).

[36] S. Samanman, P. Kanatharana, W. Chotigeat, P. Deachamag, P. Thavarungkul, Highly sensitive capacitive biosensor for detecting white spot syndrome virus in shrimp pond water, J. Virol. Methods 173 (1) (2011) 75–84.

[37] H. Im, X.-J. Huang, B. Gu, Y.-K. Choi, A dielectric-modulated field-effect transistor for biosensing, Nat. Nanotechnol. 2 (7) (2007) 430–434.

[38] J.G. Kirkwood, The dielectric polarization of polar liquids, J. Chem. Phys. 7 (10) (1939) 911–919.

[39] D.R. Lide, CRC Handbook of Chemistry and Physics, 85th Edition, CRC Press, Boca Raton, Florida, 2004.

[40] P. Wang, A. Anderko, Computation of dielectric constants of solvent mixtures and electrolyte solutions, Fluid Phase Equilibria 186 (1) (2001) 103–122.

[41] Z. Liu, J. Hu, Y. Zhao, Z. Qu, F. Xu, Experimental and numerical studies on liquid wicking into filter papers for paper-based diagnostics, Appl. Therm. Eng. (2014).

[42] T. Carpenter, E. Davies, C. Hall, L. Hall, W. Hoff, M. Wilson, Capillary water migration in rock: process and material properties examined by NMR imaging, Mater. Struct. 26 (5) (1993) 286–292.

[43] D. Lockington, J. Parlange, Anomalous water absorption in porous materials, J. Phys. D: Appl. Phys. 36 (6) (2003) 760.

[44] V. Morgan, Effects of frequency, temperature, compression, and air pressure on the dielectric properties of a multilayer stack of dry kraft paper, IEEE Trans. Dielectr. Electr. Insul. 5 (1) (1998) 125–131.

[45] A.Setayeshmehr, I.Fofana, A.Akbari, H.Borsi, E.Gockenbach, Effect of temperature, water content and aging on the dielectric response of oil-impregnated paper, in: Proceedings of the IEEE International Conference on Dielectric Liquids, ICDL, 2008, pp. 1–4.

[46] X. Huang, C. Zhi, P. Jiang, D. Golberg, Y. Bando, T. Tanaka, Temperature-dependent electrical property transition of graphene oxide paper, Nanotechnology 23 (45) (2012) 455705.

[47] M. Mraović, T. Muck, M. Pivar, J. Trontelj, A. Pleteršek, Humidity sensors printed on recycled paper and cardboard, Sensors 14 (8) (2014) 13628–13643.

[48] H. Friedenman, K.E. Shuler, Evidence for the ionic nature of certain crystal lattices, J. Chem. Educ. 24 (1) (1947) 11.

[49] S. Roberts, Dielectric constants and polarizabilities of ions in simple crystals and barium titanate, Phys. Rev. 76 (8) (1949) 1215.

[50] S. Roberts, A theory of dielectric polarization in alkali-halide crystals, Phys. Rev. 77 (2) (1950) 258.

[51] G.M. Whitesides, Cool, or simple and cheap? Why not both?, Lab Chip 13 (1) (2013) 11–13.

[52] K.A. Mirica, S.T. Phillips, C.R. Mace, G.M. Whitesides, Magnetic levitation in the analysis of foods and water, J. Agric. Food Chem. 58 (11) (2010) 6565–6569.